Numerical study of auto-ignition propagation modes in toluene reference fuel–air mixtures: Toward a better understanding of abnormal combustion in spark-ignition engines

Anthony Robert, Jean-Marc Zaccardi, Cécilia Dul, Ahmed Guerouani, Jordan Rudloff

Numerical Study of Auto-Ignition Propagation Modes in TRF-Air Mixtures: Towards a Better Understanding of Abnormal Combustion in Spark-Ignition Engines

Anthony Robert, Jean-Marc Zaccardi, Cécilia Dul, Ahmed Guerouani, Jordan Rudloff

Abstract

Two main abnormal combustions are observed in spark-ignition engines: knock and low-speed pre-ignition. Controlling these abnormal processes requires understanding how auto-ignition is triggered at the "hot spot" but also how it propagates inside the combustion chamber. The original theory regarding the auto-ignition propagation modes was defined by Zeldovich and developed by Bradley who highlighted different modes by considering various hot spot characteristics and thermodynamic conditions around the hot spot. Two dimensionless parameters (ε, ξ) were then defined to classify these modes and a so-called detonation peninsula was obtained for H_2-CO-air mixtures.

Similar simulations as those performed by Bradley et al. are undertaken to check the relevancy of the original detonation peninsula when considering realistic fuels used in modern gasoline engines. First, chemical kinetics calculations in homogeneous reactor are performed to determine the auto-ignition delay time τ_i, and the excitation time τ_e of E10-air mixtures in various conditions (calculations for a RON 95 TRF surrogate with 42.8% isooctane, 13.7% n-heptane, 43.5% toluene, and using the LLNL kinetic mechanism considering 1388 species and 5935 reactions). Results point out that H_2-CO-air mixtures are much more reactive than E10-air mixtures featuring much lower excitation times τ_e. The resulting maximal hot spot reactivity ε is thus limited which also restrains the use of the detonation peninsula for the analysis of practical occurrences of auto-ignition in gasoline engines.

The tabulated (τ_i, τ_e) values are then used to perform 1D LES of auto-ignition propagation considering different hot spots and thermodynamic conditions around them. The detailed analysis of the coupling conditions between the reaction and pressure waves shows thus that the different propagation modes can appear with gasoline and that the original detonation peninsula can be reproduced, confirming for the first time that the propagation mode can be well defined by the two non-dimensional parameters for more realistic fuels.

Keywords

Auto-ignition, Deflagration, Detonation, Fuel Reactivity, LES

Introduction

Two main abnormal combustions can be observed in modern spark-ignition engines: knock and low speed pre-ignition. Knock has been observed for the first time in 1882 by Sir Dugald Clerk who described it as a "persistent and troublesome enemy" [1] while the

first observations of low-speed pre-ignition (LSPI) date back to the beginning of years 2000 [2]. However, in both cases, the triggering and the development of the abnormal combustion process rely on the auto-ignition characteristics of the air/fuel mixture.
In order to control these abnormal phenomena, it is necessary not only to better understand how and when an auto-ignition can be triggered by "hot spots", but also how it will propagate inside the combustion chamber since the auto-ignition intensity and the potential resulting engine damages are linked to both aspects.
Different approaches such as the Livengood-Wu integral can be used to predict the auto-ignition temporal onset. However, advanced tools and methodologies are still being developed to better understand and predict the auto-ignition propagation modes.
The original theory regarding the auto-ignition propagation mode was provided by Zeldovich [3] and then developed more recently by Bradley and co-workers at Leeds University to analyze auto-ignition processes during CAI combustion [4], during knocking combustion [5], and lately during LSPI [6]. Their auto-ignition calculations for 50%H_2-50%CO-air mixtures allowed to highlight and to analyze the different propagation modes in various conditions. A specific classification diagram based on two dimensionless parameters has then been defined. Since then, this so-called "detonation peninsula" has been used for the analysis of both experimental occurrences of auto-ignition [7] and numerical results [8-9]. The recent studies of knocking combustion and LSPI require however to consider fuels whose auto-ignition characteristics are very different from those of H_2-CO.
Results obtained with n-heptane-air and isooctane-air mixtures have been recently illustrated by Bates et al. [10] but not fully compared to the original results from Gu et al. [11]. More recently, Chen et al. have thoroughly analyzed several simulation results obtained with n-heptane-air mixtures, by considering non-uniform mixture compositions, or even cool spots within the NTC region [12]. These results have highlighted the different auto-ignition propagation modes but the characteristics of n-heptane-air mixtures have not been compared to those of H_2-CO-air or TRF-air mixtures, and the detonation peninsula location has not been compared to that defined by Gu et al. [11].
This article aims at confirming the relevancy of the original detonation peninsula when considering realistic fuels used in modern gasoline engines. Similar simulations as those performed by Bradley et al. are reported in this article but the novelty lies in the use of a TRF surrogate fuel featuring very different auto-ignition characteristic time scales as those of H_2-CO. The first section introduces the main features of the original theory allowing to characterize the auto-ignition propagation mode. The second section introduces the numerical procedure used to reproduce the different auto-ignition propagation modes. The third section focuses then on the fuel reactivity. It discusses the expected impacts on the shape and location of the detonation peninsula when considering the auto-ignition characteristic time scales and diffusion properties of a realistic complex fuel. The fourth and fifth sections finally presents the 1D numerical setup and the simulation results obtained with various hot spots and thermodynamic conditions.

Theoretical background

Auto-ignition in Spark Ignition (SI) engines appears randomly in time during the engine cycle, after the spark in the case of knocking combustion, or before in the case of LSPI.

Regarding its location, auto-ignition is triggered in reactive centers resulting from mixture heterogeneities inside the combustion chamber. These heterogeneities can be linked to higher temperatures, to the local mixture composition featuring an increased reactivity (local fuel/air and dilution ratios), or even to external perturbations like solid particles or oil droplets. It is usually assumed, however, that reactive auto-ignition centers correspond to temperature gradients within the mixture, that is why these are often called "hot spots".

Two kinds of waves are generated when auto-ignition is triggered: a reaction wave associated with the chemical propagation of the reactive front and a pressure wave initiated by the thermal explosion of the hot spot at the very beginning of auto-ignition. If the local overpressure generated at the moment of auto-ignition is strong enough to provide a critically short auto-ignition delay time in the surrounding mixture, the reactive front and the pressure wave may couple and form a detonation wave, which propagates throughout the mixture. Both waves are intrinsically linked, since the compression of the mixture close to the hot spot contributes to an increase in reactivity and propagates auto-ignition.

Zeldovich [3] showed that a one-dimensional thermal hot spot characterized by its radius and by its temperature gradient between its center and the surrounding mixture can lead to four kinds of auto-ignition propagation modes. The first case corresponds to a supersonic auto-ignition with a reaction wave propagating ahead of the pressure wave. In Zeldovich's classification thermal explosions represent a limit case of supersonic auto-ignition with an infinite propagation speed of the reactive front. The second one corresponds to the stationary detonation for which the shock wave compresses the unburned gas ahead of it, thereby supporting and reinforcing the chemical reaction. The pressure and the reaction waves have thus the same speed which is theoretically the Chapman-Jouguet speed. Both waves continuously interact and amplify each other, resulting in high local pressure levels. Finally, the third and the fourth modes concern subsonic auto-ignition propagations, one with the reaction wave faster than the laminar flame speed and the other with the reaction wave slower, so that normal flame propagation driven by the laminar flame speed occurs. The different flame propagation modes issued from auto-ignition are widely discussed in literature [4-12].

This original theory has then been further developed and applied to the analysis of auto-ignition in internal combustion engines by D. Bradley and his co-workers at the University of Leeds [4-6,11]. A specific numerical methodology has been developed to determine the auto-ignition propagation mode around a one-dimensional thermal hot spot characterized by its radius r_0 and by its temperature gradient between its center and the surrounding mixture $\partial T/\partial r$. Two dimensionless parameters (ε,ξ) were defined depending on the hot spot characteristics and on the surrounding fresh gas mixture properties (pressure, temperature, fuel/air equivalence ratio, dilution ratio).

ξ describes the coupling between the acoustic wave propagating at the speed of sound a, and the reaction wave propagation at the speed u_a. It can be written as a dimensionless temperature gradient considering the temperature gradient between the center of the hot-spot and the surrounding mixture, and the auto-ignition delay τ_i (Eq. 1).

$$\text{Eq. 1} \quad \xi = \frac{a}{u_a} = \frac{a}{\partial r/_{\partial \tau_i}} = \frac{a}{\partial r/_{\partial T} . \partial T/_{\partial \tau_i}}$$

ξ can also be written as a dimensionless temperature gradient by defining a critical hot spot temperature gradient (Eq. 2) for which the chemical resonance between the pressure wave and the reaction front occurs.

$$\text{Eq. 2} \quad \xi = \left(\partial T/\partial r\right) \cdot \left(\partial T/\partial r\right)_c^{-1} \text{ with } \left(\partial T/\partial r\right)_c = a^{-1} \cdot \left(\partial \tau_i/\partial T\right)^{-1}$$

Theoretically, detonation is achieved as soon as the reaction and pressure waves propagate at the same speed (ξ = 1, [13]). However, because of species and thermal diffusion during the induction period, a developing detonation is not stringently restricted to this critical value ξ = 1. In fact, depending on the reactivity, a wider range of initial conditions can lead to a developing detonation. Thus, an upper limit ξ_u and a lower limit ξ_l have been introduced to classify the different propagation modes and to define a so-called detonation peninsula.
The second dimensionless parameter ε compares the characteristic chemical time scale given by the excitation time τ_e, and the acoustic time scale given by r_0/a (Eq. 3). By quantifying the rate at which the auto-ignition chemical energy is released into the acoustic wave, ε measures the hot spot reactivity.

$$\text{Eq. 3} \quad \varepsilon = \frac{r_0/a}{\tau_e}$$

It must be noted that ε and ξ are determined as a function of initial conditions (before chemical reactions start). Usually, characteristics of the fresh gas needed to determine ξ and ε can be directly known (pressure, fuel/air ratio) or derived (temperature and dilution) from experimental data or simulations. However, the thermal hot spot properties (radius and temperature gradient) must be assumed.
Lots of recent studies used this detonation peninsula to analyze experimental and numerical occurrences of knock and LSPI in highly charged SI engines. Based on this classification diagram, it has been shown that a developing detonation mode may appear under extreme conditions. It is therefore essential to validate the location of this peninsula.

Numerical procedure

The first step to estimate ε and ξ in our 1D calculations consists in calculating the auto-ignition characteristic time scales (τ_i, τ_e) of fuel-air mixtures by performing chemical kinetics calculations. The auto-ignition delay time τ_i is defined as the time needed to increase the mixture temperature by 400K compared to the initial conditions. The excitation time τ_e is the time required for the heat release rate to rise from 5% to its maximal value. This characteristic time being of the order of µs, a high temporal resolution is required for the post-processing to guarantee accurate calculations.

Involving a complex chemical mechanism in numerical codes to solve chemistry of realistic fuels requires computing thousands of species and reactions, and is too CPU time consuming as the objective of this work is to analyze a large number of operating conditions to precisely define the detonation peninsula. The tabulated model TKI-LES model [14] has thus been chosen to simulate auto-ignition as previous studies have already shown its ability to catch such phenomenon [15]. This model is based on a look-up table of τ_i and τ_e, obtained using a priori calculations for a surrogate fuel in homogeneous reactors and considering the LLNL kinetic mechanism with 1388 species and 5935 reactions. The chemical computations are first performed with an in-house code named CLOE (based on the Senkin solver), and the resulting auto-ignition characteristic time scales (τ_i, τ_e) are then tabulated for different pressure and temperature levels. The values of τ_i and τ_e are just read in the table during the 1D calculations.

Fuel reactivity

Contrary to previous studies of Bradley et al. which are based on H_2-CO-air mixtures, this work focuses on the study of a complex fuel, namely the European standard fuel E10. It is important to notice that even if this fuel can include up to 10% of volume fraction of ethanol, its RON remains around 95. A fuel surrogate and a kinetic mechanism including ethanol have been previously used by the authors to study the auto-ignition propagation modes [7]. These first investigations had been performed for E5 and E10 fuels and the comparison of the auto-ignition characteristic time scales τ_i and τ_e had not shown any significant difference.

Based on the conclusions of [7], a Toluene Reference Fuel (TRF) surrogate has been defined with 42.8% isooctane, 13.7% n-heptane and 43.5% toluene [16].The choice of this specific TRF without ethanol is due to the surrogate definition methodology used by the authors [16]. Surrogate is defined to achieve similar characteristics as the reference fuel in terms of RON, MON, LHV and composition. In these works, the objective is to well represent the fuel auto-ignition characteristics so weighting to the RON and MON targets that is 10-times greater than those allocated to the fuel composition. In addition, the fuel oxygen-to-carbon ratio impacts the lower heating value and the fuel-air stoichiometric ratio, but to a much lesser extent the auto-ignition properties. The TRF surrogate can thus be considered as a good representative of a 95 RON E10 fuel in terms of auto-ignition properties.

This preliminary study aims at analyzing the fuel impact on critical (ε,ξ) values and on the potential modification of the location of the original detonation peninsula. Fig. 1 compares the auto-ignition delay times and excitation times calculated for TRF-air mixtures to those obtained for 50%H_2-50%CO-air mixtures. The comparison has been focused on temperatures below 1100 K at which auto-ignition usually occur in SI engines (either during knocking combustion or LSPI).

The critical temperature gradients leading to ξ = 1 for both fuels have first been compared to know if the required theoretical conditions for detonation are similar or not (Eq. 2). Fig. 1 (a) shows that the critical temperature gradients can be much higher for TRF-air mixtures than for H_2-CO-air mixtures below 1100 K. A hot spot having a critical temperature gradient when considering H_2-CO-air mixtures is thus not critical when

considering TRF-air mixtures. At 50 bar and 1100 K for example, a critical temperature gradient of around 2.73 K/mm is obtained for 50%H_2-50%CO-air mixtures but in the case of TRF-air mixtures this temperature gradient would lead to $\xi \approx 0.50$ (the critical temperature gradient for TRF-air mixtures being around 5.44 K/mm). In this case, the dangerous detonation propagation mode should thus be avoided in favor of a supersonic deflagration mode. For a given temperature gradient at the hot spot, these two fuels will thus lead to very different ξ values. More generally, depending on the mixture's properties and on the chosen temperature gradient around the hot spot, a modification of the vertical position of the detonation peninsula can therefore be expected when considering TRF-air mixtures.

This comparative analysis is performed here by considering that the two fuels only differ in their auto-ignition delay times τ_i. However, the induction period is particularly essential to determine the auto-ignition propagation mode because of the mixture's homogenization around the hot spot during this period. Indeed, mixtures leading to long auto-ignition delay times, and those characterized by strong species and thermal diffusion properties around the hot spot will then allow the mixture to well homogenize before auto-ignition is triggered. As a consequence, the critical ξ values defining the limits between developing detonation and deflagrations might change when considering different fuels.

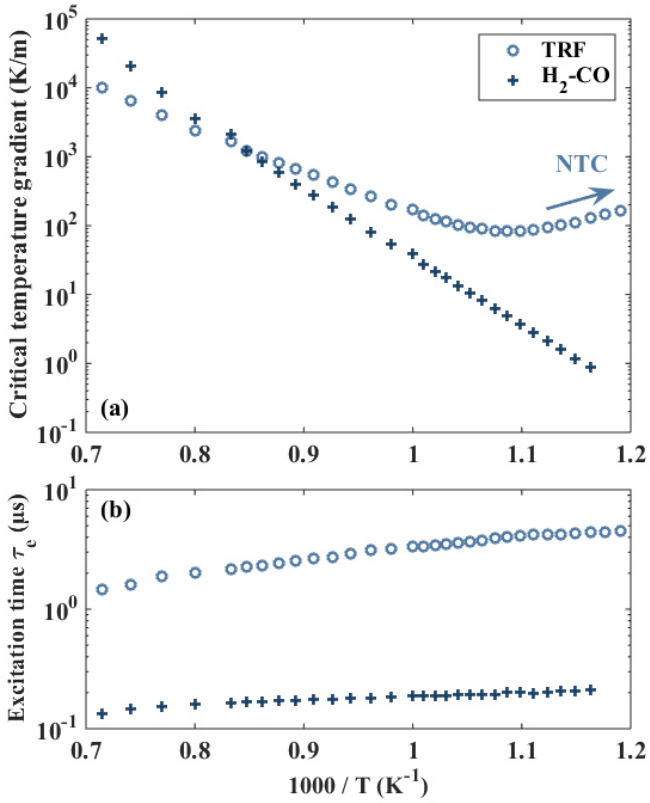

Fig. 1: Critical temperature gradients (a) and excitation times (b) computed for 50%H_2-50%CO-air and TRF-air mixtures at 50 bar (stoichiometric conditions, no dilution).

By comparing the two fuels, it is also observed that excitation times of 50%H_2-50%CO-air mixtures are ten to twenty times lower than those of TRF-air mixtures below 1100 K (see Fig. 1 (b)). Usually, in order to calculate ε, r_0 values between 1 and 5 mm are chosen as representative values for turbulent flow length scales and heterogeneities in SI engines. However, since excitation times of TRF-air mixtures are much higher than those of H_2-CO-air mixtures, it is necessary to assume very large hot spot radii r_0 for TRF-air mixtures in order to reach the same ε values with both fuels. For example, considering H_2-CO-air mixtures at 50 bar and 1100 K, a hot spot radius of 1.2 mm can lead to $\varepsilon \approx 10$ (which can be considered as a meaningful limit value defining the steep transition between subsonic deflagration and detonation for ξ varying from 10 to 40 [4]). In the same conditions, a radius of around 15 mm is needed to reach the same ε with TRF-air mixtures, which is not relevant to analyze auto-ignition in SI engines. Based on the computed τ_e values, it has been found that reasonable hot spot radii below 10 mm can lead to $\varepsilon \approx 10$ only at very high temperature and pressure levels. Consequently, if this analysis methodology based on a single thermal hot spot is considered and if the original detonation peninsula can be used for TRF-air mixtures, then the use of this peninsula should be limited to $\varepsilon \approx 10$ (accordingly with recently reported analyses of LSPI events [10]).
The second important conclusion from this comparative analysis is that it is essential to calculate τ_e as precisely as possible. Indeed, as a function of the assumptions used to define the hot spot, the accuracy of the chemical kinetics calculations greatly influence the location of the points in the detonation diagram (as it has been shown in [7] by comparing two chemical schemes).

Numerical set-up

To analyze auto-ignition behavior, one dimensional calculations are performed using the AVBP code [17]. The computational domain is presented in Fig. 2.

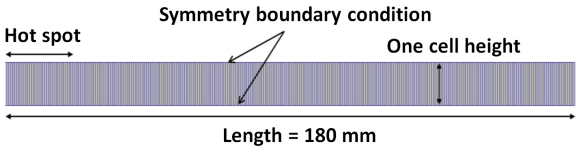

Fig. 2: Calculation domain.

A grid convergence has been achieved using cells down to 6 µm and the final mesh used for all calculations owns 3600 cells for a length of 180 mm, which corresponds to cells of 50 µm.
To mimic the hot spot, a linear temperature gradient is initialized on the left part of the domain with a defined amplitude and radius. Fig. 3 illustrates this simplified configuration for the general case where T_0 is chosen outside of the NTC region where τ_i increases as T decreases.

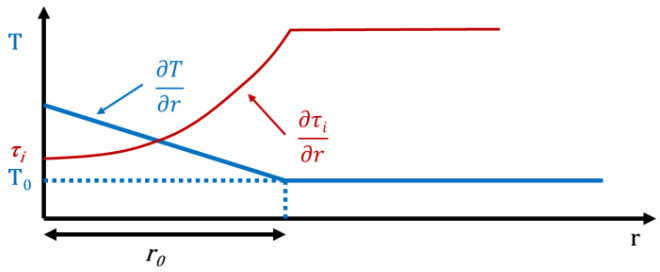

Fig. 3: Initial hot spot definition.

A "symmetry" boundary condition is used at the center of the hot spot (left part of the domain) and a constant pressure boundary condition is defined at the outlet.

Regarding the initial conditions, the domain is fueled using a stoichiometric mixture without any dilution. All the calculations presented here are performed with an initial pressure P_0 of 50 bar and an initial temperature T_0 of 1100 K. This initial temperature corresponds to high temperature reactions and is higher than the classical fresh gases temperature that can be achieved in SI engines when auto-ignition is triggered (whether during classical knocking combustion or LSPI). However, this initial temperature condition has been chosen here to compare the obtained results with those already available in the literature [9][11]. Realistic operating conditions corresponding to knocking combustion or LSPI would rather lead to initial temperature conditions in the range of 700 to 900 K.

It must be noted that the reactivity and coupling parameters (ε, ξ) are defined using the initial conditions of the domain. Referring to the original works of Gu and Bradley, the reference initial temperature at $r = r_0/2$ is used to determine τ_i and τ_e, then used to calculate ε and ξ. The choice of the reference temperature location has a significant impact on the calculation of (ε, ξ) values. Fig. 4 shows the variations of these parameters as a function of the temperature increase at the center of the hot spot ΔT_0, for three hypotheses: when the reference temperature is taken at the outer limit of the hot spot (assumption n°1, $r = r_0$), at the middle of the hot spot (assumption n°2, $r = r_0/2$), and at the center of the hot spot (assumption n°3, $r = 0$).

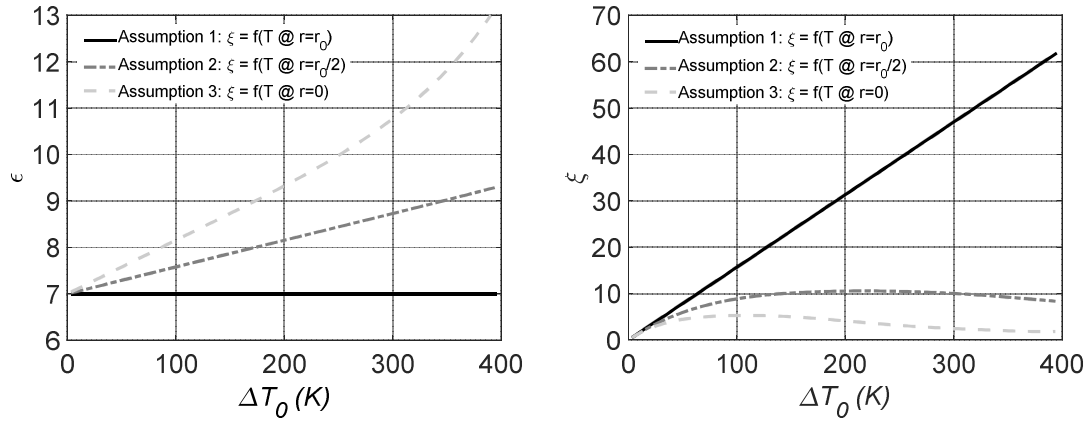

Fig. 4: Impact of the reference temperature on ε (top) and ξ (bottom) values as a function of ΔT_0 at the center of the hot spot (r_0 = 12.1 mm, P_0 = 50 bar, T_0 = 1100 K, ϕ = 1, no dilution).

For the highest ΔT_0, the estimation of the two parameters varies a lot for the same initial conditions, meaning that the position on the detonation peninsula can be totally different. For example, Table 1 summarizes the ε and ξ values obtained by considering these three different assumptions for the same hot spot configuration with a temperature increase ΔT_0 of 100 K. The impact on ε is rather limited but the impact on ξ values is really significant. For these conditions, a subsonic deflagration can clearly be expected according to assumption n°1, but assumption n°3 would indicate a developing detonation.

Table 1: Impact of the reference temperature on (ε, ξ) values for ΔT_0 = 100 K (r_0 = 12.1 mm, P_0 = 50 bar, T_0 = 1100 K, ϕ = 1, no dilution).

Assumption	ε	ξ
1: T @ $r = r_0$	7.0	15.7
2: T @ $r = r_0/2$	7.6	8.9
3: T @ $r = 0$	8.1	5.3

For the fuel sensitivity analysis conducted here, a proper comparison with the original detonation peninsula provided by Gu and Bradley can only be achieved if a similar assumption is made regarding the choice of the reference temperature. The estimation of (ε, ξ) at $r = r_0/2$ is used for the following cases.

Results

A large number of hot spot configurations are simulated in order to ascertain the relevancy of the original detonation peninsula when considering a realistic commercial fuel. The methodology consists in defining values for ε and ξ, and then to deduce the

initial characteristics of the hot spot. Based on Eq. 3, the initial radius r_0 of the hot spot is given by Eq. 4.

$$\text{Eq. 4} \quad r_0 = a \cdot \varepsilon \cdot \tau_e$$

whereas the initial temperature gradient is obtained based on Eq. 1 with Eq. 5.

$$\text{Eq. 5} \quad {}^{\partial T}/_{\partial r} = \frac{\xi . {}^{\partial T}/_{\partial \tau_i}}{a}$$

Several hundreds of calculations have been performed for ε and ξ respectively ranging from 1 to 17, and from 1 to 38 for both parameters. This large number of calculations have been performed in order to define as precisely as possible the location of the transition zone between deflagration and developing detonation.

To illustrate the potential of such numerical simulations, five different cases are first analyzed. Their assumed positions in the original detonation diagram are presented in Fig. 5. The first objective is to determine whether the assumed (ε,ξ) values for these five cases lead to case A in the subsonic deflagration zone, cases B and C at the limit of the detonation peninsula, case D in detonation zone and case E in the supersonic deflagration zone. Cases B and C correspond not only to a transition zone between the deflagration and the developing detonation, but also to operating conditions representative of those in which auto-ignition can occur in spark-ignition engines [6, 7, 15]. On the contrary, no realistic engine operating conditions should lead to case E. However, this case is shown here to demonstrate that our numerical methodology and tools can reproduce the different propagation modes.

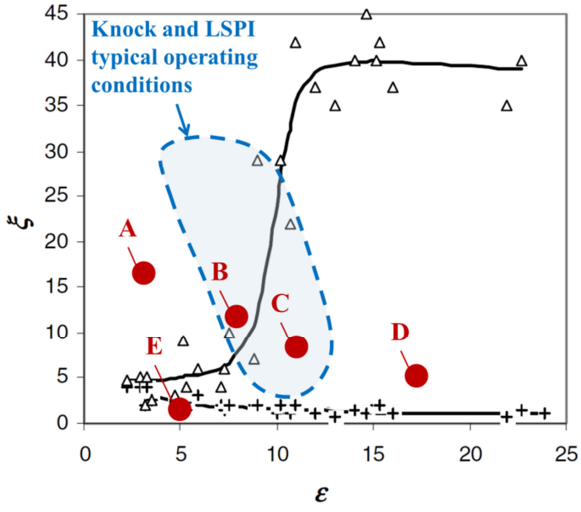

Fig. 5: Position of analyzed conditions in the original detonation peninsula [4].

The characteristic parameters for the corresponding hot spots are summarized in Table 2.

Table 2: Hot spots characteristics for the five cases.

Case	ε	ξ	r_0 [mm]	$\partial T/\partial r$ [K/mm]
A	3.1	16	5.2	10.8
B	7.9	10.7	12.2	10.8
C	11.1	8.7	15.7	10.8
D	16.9	5.4	22.7	10.8
E	5	1	8.7	0.54

In the following sections, the auto-ignition propagation modes are analyzed for these five different cases.

Case A, $\varepsilon = 3.1$, $\xi = 16$

According to the original detonation diagram obtained with H_2-CO-air mixtures, case A should correspond to a subsonic deflagration mode. Results obtained with the TRF-air mixture confirm this propagation mode as it can be seen in Fig. 6 with the pressure and temperature profiles given for different timings up to t = 0.190 ms (τ_i = 0.286 ms for the considered operating conditions). The pressure wave is distinctly propagating much faster than the reaction wave since the temperature increase in the computational domain is obviously slower than the pressure increase. The pressure wave intensity remains also quite limited, the maximal pressure being of the order of 63 bar. In those conditions, the deflagration propagation mode is well reproduced by the 1D calculations performed with the TRF.

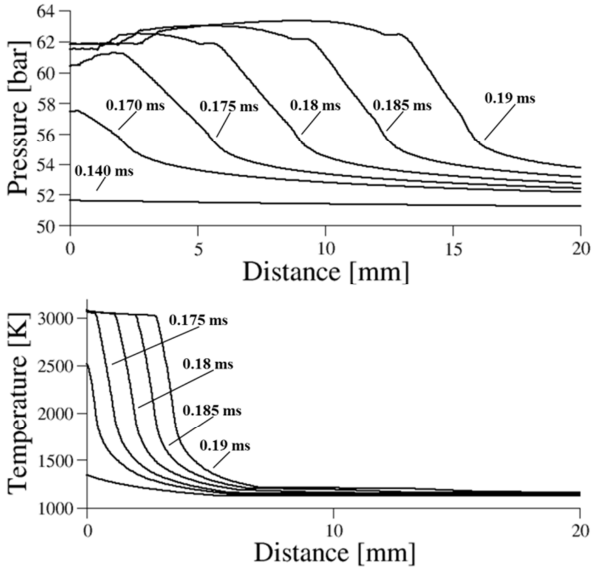

Fig. 6: Hot spot auto-ignition for case A (r_0 = 5.2 mm, ΔT_0 = 56.2 K, ε = 3.1, ξ = 16, P_0 = 50 bar, T_0 = 1100 K, ϕ = 1, τ_i = 0.286 ms). Time sequence from 0.14 ms up to 0.190 ms.

Case B, $\varepsilon = 7.9$, $\xi = 10.7$

Considering the original detonation peninsula, the case B should be located close to the transition zone between the subsonic deflagration and developing detonation modes. Indeed, it must be mentioned that the limit between these two modes is not clearly defined by a single line, and that a transition zone exists since it takes some time for the pressure and the reaction waves to couple.
Results obtained with the TRF-air mixture are illustrated in Fig. 7 for different timings up to $t = 0.11$ ms ($\tau_i = 0.286$ ms).

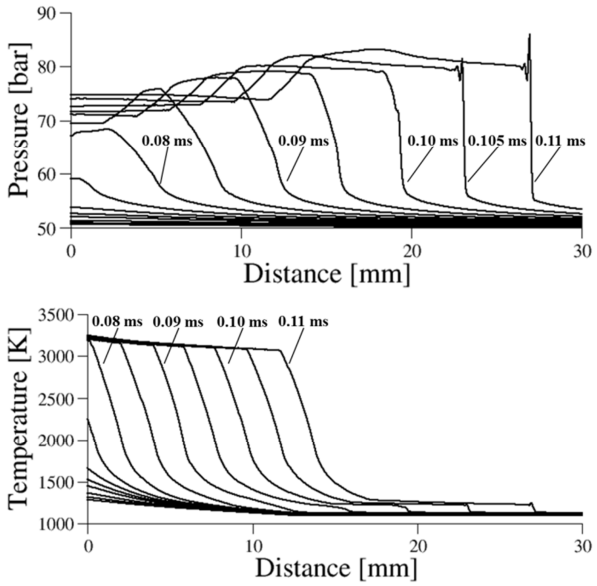

Fig. 7: Hot spot auto-ignition for case B ($r_0 = 12.2$ mm, $\Delta T_0 = 131.8$ K, $\varepsilon = 7.9$, $\xi = 10.7$, $P_0 = 50$ bar, $T_0 = 1100$ K, $\phi = 1$, $\tau_i = 0.286$ ms). Time sequence from 0.03 ms up to 0.11 ms.

The analysis of the auto-ignition development shows that the pressure front is steeper than in the case A, and that the pressure wave is still propagating ahead of the reaction wave. This case corresponds thus once again to a subsonic deflagration even if both pressure and reaction waves propagate faster outside the hot spot (r_0 = 12.2 mm) in comparison with the case A. In addition, the pressure wave intensity is higher than for the case A, the maximal pressure being of the order of 85 bar. Indeed, an amplification of the pressure wave is observed here which points out a more intense auto-ignition reaction and an interaction between the pressure and the reaction waves. These various intensities in the subsonic deflagration regime can explain the various knocking intensities that can be experimentally observed. Indeed, the difference between light and moderate knocking cycles might not be due different auto-ignition propagation modes (deflagration or detonation) but more simply to subsonic deflagrations having different intensities.

A sharp peak pressure also appears at t = 0.105 ms, which points out the beginning of the transition towards a thermal explosion as it will be shown later with the analysis of the reaction wave speed.
At this point, the calculations performed with TRF-air mixtures still confirm the location of the original detonation peninsula.

Case C, $\varepsilon = 11.1$, $\xi = 8.7$

According to the original detonation peninsula, case C should be located as well in the transition zone between the subsonic deflagration and the developing detonation mode. The auto-ignition process illustrated in Fig. 8 shows that the coupling between the pressure and reaction waves tends to establish itself, but these waves are still not perfectly synchronized. The pressure increase within the hot spot is higher than for cases A and B thanks to the spatial proximity of the pressure and reaction fronts but the conditions required for a detonation are still not met. However, the pressure front becomes much steeper as soon as the reaction exits the hot spot (r_0 = 15.7 mm). In this case C, the pressure wave intensity is much higher than for case B with a maximal pressure of around 220 bar.
The results for t > 0.085 ms are not shown here because no real coupling of the pressure and reaction waves can be observed before they reach the end of the computational domain.

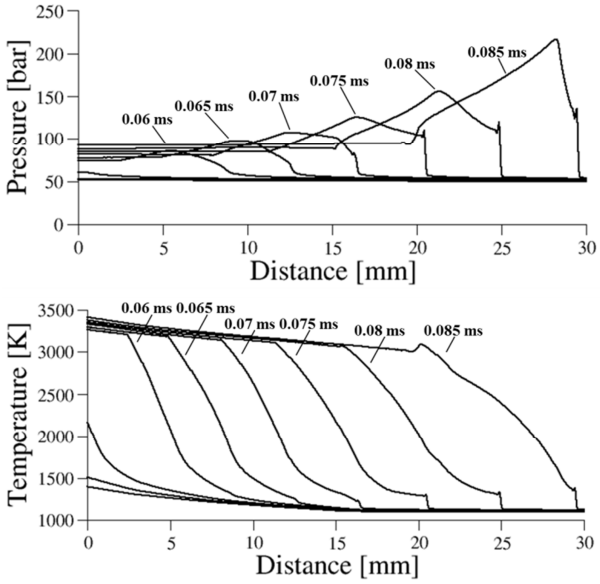

Fig. 8: Hot spot auto-ignition for case C (r_0 = 15.7 mm, ΔT_0 = 169.6 K, ε = 11.1, ξ = 8.7, P_0 = 50 bar, T_0 = 1100 K, ϕ = 1, τ_i = 0.286 ms). Time sequence from 0.030 ms up to 0.085 ms.

The comparative analysis of cases B and C shows that the increased reactivity achieved with the larger hot spot radius allows to confirm the location of the transition zone

between the subsonic deflagration and the developing detonation modes even when using a Toluene Reference Fuel.

Case D, $\varepsilon = 16.9$, $\xi = 5.4$

The last case D (see Fig. 9) allows to observe a gradual coupling of the pressure and reaction waves after they exit the hot spot (r_0 = 22.7 mm). This coupling is still not perfect as the pressure wave is still increasing at t = 0.06 ms meaning that the detonation regime is not fully established.

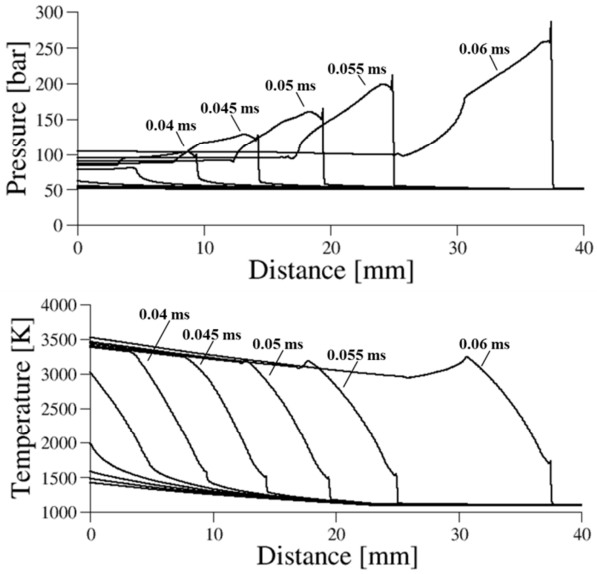

Fig. 9: Hot spot auto-ignition for case D (r_0 = 22.7 mm, ΔT_0 = 245.2 K, ε = 16.9, ξ = 5.4, P_0 = 50 bar, T_0 = 1100 K, ϕ = 1, τ_i = 0.286 ms). Time sequence from 0.01 ms up to 0.06 ms.

However, the temperature and pressure fronts are very steep and propagate at the same speed. As a consequence, the pressure and reaction wave reinforce themselves and the pressure peaks reach extreme values above 250 bar. Much higher pressure levels above 350 bar can be reached in some cases even when considering small heterogeneities in terms of amplitude and radius, namely in the lower left toe of the detonation peninsula (ε lower than 10, ξ lower than 5).

This case D is quite extreme since it requires the use of a large hot spot to enhance the mixture's reactivity (r_0 = 22.7 mm). This radius is much too large to be representative of realistic mixture heterogeneities in SI engines and, accordingly, these (ε, ξ) values have not been reported so far as being representative of auto-ignitions observed in SI engines (see Fig. 5).

The results obtained here with case D show first that the simulation methodology is capable of catching such a detonation phenomenon, and also confirm once again that the

developing detonation mode that can be forecasted with the original peninsula is confirmed when using a Toluene Reference Fuel.

Case E, $\varepsilon = 5$, $\xi = 1$

Case E is a specific case study that is detailed here to show that the calculation methodology can reproduce all the possible propagation modes. Low ε and ξ values are considered for this example, but these operating conditions are clearly out of scope for the analysis of realistic knocking and LSPI events (see Fig. 5).

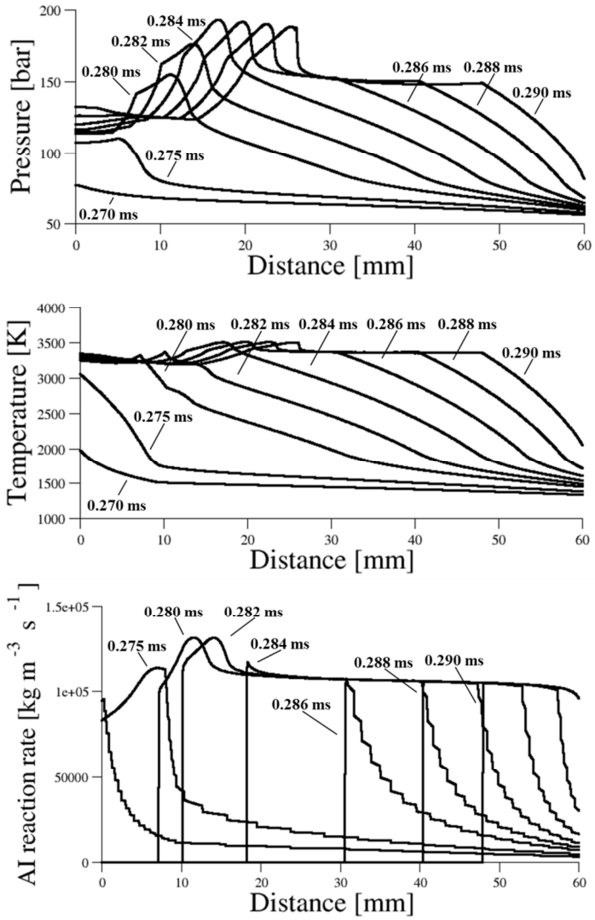

Fig. 10: Hot spot auto-ignition for case E (r_0 = 8.7 mm, ΔT_0 = 4.7 K, ε = 5, ξ = 1, P_0 = 50 bar, T_0 = 1100 K, ϕ = 1, τ_i = 0.286 ms). Time sequence from 0.270 ms up to 0.290 ms.

Pressure and temperature profiles shown in Fig. 10 focus on the very last stages of the calculation, starting at t = 0.270 ms up to t = 0.290 ms. The auto-ignition reaction rate is also plotted in the lower part of Fig. 10 to better highlight the reaction wave propagation. During this short period of time, a transition from a supersonic deflagration to a thermal

explosion can be observed. Up to t = 0.282 ms, the reaction wave propagates slightly faster than the pressure wave and also that no sharp pressure peaks can be observed contrary to a developing detonation case. The maximal pressure levels rise up to 200 bar, which is higher than for subsonic deflagration but still lower than for developing detonations.
Then, from t = 0.282 ms, the reaction rate becomes homogeneous in the unburned gases zone and a thermal explosion takes place. Because of this homogeneous reaction, the pressure levels are increased but not as high as in the case of developing detonations (see Fig. 9).
Surprisingly, Fig. 10 shows that no thermal explosion is observed at t = 0.286 ms which corresponds to the expected auto-ignition delay time τ_i at 50 bar and 1100 K. This can be explained by the local auto-ignition delay time that is slightly increased by around 4 µs close to the outlet of the computational domain because of the static pressure imposed as outlet boundary condition. Consequently, the thermal explosion is not observed at $t = \tau_i$ = 0.286 ms but just after t = 0.290 ms (not shown here).

To clarify the different propagation modes, Fig. 11 shows the reaction wave speed for the five different cases. These reaction wave speeds are plotted along the computational domain as a function of the hot spot radii that were used for the calculations.

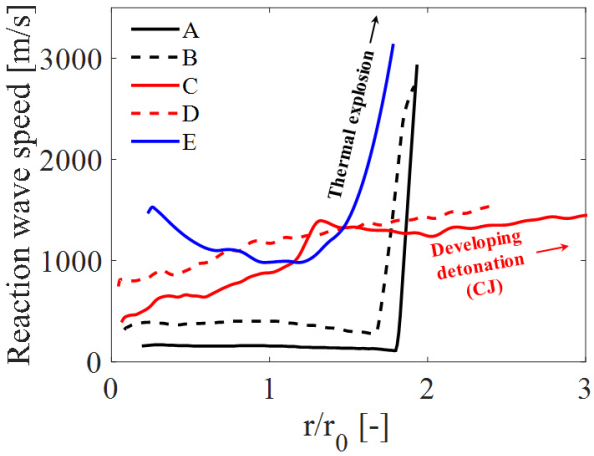

Fig. 11: Reaction front wave speed.

The reaction wave speed for case A remains very low around 100 m/s until it reaches r/r_0 ≈ 1.7 (with r_0 = 5.2 mm for case A). At that point, the reaction wave speed is sharply increasing because of the homogeneous auto-ignition in the whole domain which corresponds to the final transition towards a thermal explosion [3-4]. A similar process can be observed for case B with a reaction wave speed around 370 m/s up to $r/r_0 \approx 1.8$. In this case, the thermal explosion occurs thus when the reaction wave is propagating beyond a distance from the center of the hot spot of around 20 mm.
For cases C and D, the reaction wave speeds increase as the coupling with the pressure wave is establishing. The reaction speed is thus getting closer and closer to the theoretical Chapman-Jouguet detonation speed above 1500 m/s. The computational domain is not

long enough to reach a perfect coupling between the pressure and the reaction waves. It is, however, already way too long compared to the characteristic size of the unburned gases zone in SI engines. Consequently, if it is difficult to achieve a perfect coupling in those very favorable conditions combining a long computational domain and a high mixture's reactivity (T_0 = 1100 K), obtaining a stabilized detonation in SI engines will be even more questionable.
Finally, a fast reaction wave can be observed for case E. the reaction wave speed is already higher than 1000 m/s at the beginning of combustion for $r/r_0 < 1$. Then, as shown by Fig. 11, a thermal explosion occurs as soon as the reaction wave propagates beyond x ≈ 15 mm ($r/r_0 > 1.5$).

Detonation peninsula for TRF-air mixtures

Given the large amount of calculations carried out, an automated post-processing has been set up to quickly identify the auto-ignition propagation modes for all the simulated (ε, ξ) values. However, this detection process is not straightforward and requires to define two main criteria.
The first criterion indicates if the pressure wave and reaction wave fronts are coupled or not. The second criterion indicates how far from the hot spot center, or how long after the beginning of auto-ignition the identification of the propagation mode should be performed. Indeed, even a simple subsonic deflagration can be allowed to degenerate into a thermal explosion (as shown for example by cases A and B in Fig. 11). It is therefore essential to decide on the nature of the propagation mode before this thermal explosion is triggered. In other more complex cases, it is even possible to observe a complete evolution of the propagation mode from a subsonic deflagration to a developing detonation which, depending on the conditions, may stabilize for some time, or quickly degenerate into a supersonic deflagration or a thermal explosion [11]. The second criterion allows to face these various situations by defining the spatial position where the identification of the auto-ignition propagation mode is performed when the pressure and reaction waves arrive at this position.
Several post-processing variants have been tested and others are still being evaluated, with the objective of identifying the propagation mode in an automatic but above all robust way. It must can be noted that the definition of precise limits for the peninsula is not always required or even necessarily possible because various transition phenomena can occur.
Fig. 12 shows the original detonation peninsula (black lines) [4], the entire domain that could be investigated with TRF-air mixtures (blue region) and the limits (red dot lines) obtained with those new 1D calculations. For these results, the post-processing procedure is based upon the analysis of the relative position and velocity of the reaction and pressure waves. The analysis is carried out at the moment when the reaction wave reaches $r = r_0$, just before the reaction begins its propagation into a perfectly homogeneous mixture. Theoretically, the detonation mode is reached when the positions and speeds of the reaction and pressure fronts perfectly coincide. However, a tolerance of 10% is used here on speed and position in order to take into account transition phenomena during which pressure and reaction fronts chase each other. The criteria used

to differentiate the main modes of propagation are summarized in Table 3 as a function of the reaction and pressure wave speeds and positions (respectively noted here u_a, x_a, a, x_p).

Table 3: Identification criteria for auto-ignition propagation modes.

	Reaction front speed u_a	Reaction front position x_a
Developing detonation	$0.9*a < u_a < 1.1*a$	$0.9*x_p < x_a < 1.1*x_p$
Subsonic deflagration	$u_a \leq 0.9*a$	$x_a \leq 0.9*x_p$
Supersonic deflagration	$u_a \geq 1.1*a$	$x_a \geq 1.1*x_p$

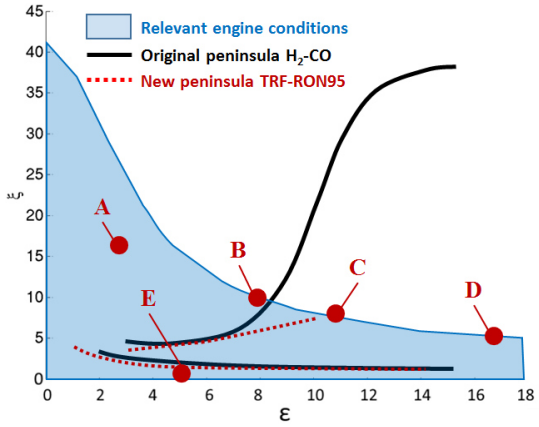

Fig. 12: Detonation peninsula calculated for TRF-air mixtures (P_0 = 50 bar, T_0 = 1100 K, ϕ = 1, no dilution).

The first observation is that the region described with our TRF is much limited compared to the one obtained with a H_2-CO fuel. Indeed, the parameter ε depends on τ_e (Eq. 3) which varies a few when changing the temperature of the hot spot (Fig. 1, bottom). Looking at parameter ξ, Eq. 2 points out that it is linked to the critical temperature gradient, and Fig. 1 confirms a strong variation when temperature increases. The behavior of the critical temperature gradient between the two fuels is different, and explains the maximal low values of ξ reached at high values of ε.

This new peninsula obtained with TRF-air mixtures is close to the original one which shows that the auto-ignition propagation mode can be well predicted by the two dimensionless parameters ε and ξ even if the auto-ignition characteristic time scales τ_i and τ_e are very different for both fuels.

In these works, a particular attention has been paid to the definition of the transition zone between subsonic deflagration and developing detonation for the operating conditions representative of those in which auto-ignition can occur in spark-ignition engines (see Fig. 5). Fig. 12 shows that this transition occurs somewhere in between cases B and C characterized by hot spot radii of 12.2 and 15.7 mm respectively. It has to be kept in mind that there is no clear demarcation line between deflagration and developing detonation that is why case C is considered as a detonation case by our automatic post-processing

methodology in Fig. 12, while the detailed analysis reported in Fig. 8 shows that the detonation is not really established even if the conditions are favorable.
As mentioned above, high hot spot radii higher than that of case C (r_0 = 15.7 mm) are required to reach the developing detonation mode because of the high excitation times values of TRF-air mixtures in comparison with those of H_2-CO-air mixtures (see Fig. 1). However, these radii being much higher than the turbulent flow and heterogeneities characteristic length scales in SI engines, it can be argued whether a developing detonation could really be observed in realistic engine operating conditions with a standard gasoline fuel.

Conclusions

A numerical procedure has been set up to simulate the propagation of auto-ignition originating from a one-dimensional thermal hot spot. By combining chemical kinetics calculations and the TKI-LES model, all the possible propagation modes can be reproduced and the original detonation peninsula originally defined for 50%H_2-50%CO can be almost reproduced with a TRF surrogate representative of a realistic gasoline fuel. These works confirm thus that the propagation modes can be well defined by the two dimensionless parameters (ε, ξ) when studying auto-ignition in SI engines running on gasoline fuel. It has also been shown that the use of the detonation peninsula should be limited to $\varepsilon \approx 10$. Indeed, the excitation times of TRF-air mixtures being much higher than those of H_2-CO-air mixtures, higher values of ε should not be reached when assuming relevant hot spot radii for the analysis auto-ignition in SI engines. It should be noted, however, that this methodology is based on the assumption of a single hot spot, while multiple hot spots interacting with each other should be considered for the analysis of realistic engine conditions.

The current activities focus now on the automated post-processing methodology in order to accurately complete the definition of the new peninsula for TRF-air mixtures. Even if different criteria can be used to determine the auto-ignition propagation mode, it is important to note that the definition of exact boundaries between the different propagation modes is not required because of the assumptions made for the hot spot radius and temperature gradient.
Additional works are also needed to confirm the peninsula's location when varying the mixture's characteristics according to realistic local conditions in SI engines (notably the fresh gases temperature, the fuel/air and dilution ratios). These new results will be published in an upcoming publication in 2018.
The combination of a reliable peninsula and 3D CFD engine calculations will then allow to study more precisely the impacts of mixture's heterogeneities and of the interactions between hot spots and the combustion chamber walls. The better understanding of auto-ignition propagation modes will thus allow to optimize future highly efficient internal combustion engines concepts mixing controlled flame propagation and auto-ignition processes such as Spark-Assisted Compression Ignition.

ACKNOWLEDGEMENTS

The authors would like to thank M. Matrat, A. Dulbecco, C. Angelberger and O. Colin for their support and comments.

FUNDING

The authors received no financial support for the research reported in this article.

NOMENCLATURE

τ_i	auto-ignition delay time
τ_e	excitation time
ε	hot spot reactivity
ξ	coupling parameter
$\left(\partial T/\partial r\right)$	hot spot temperature gradient
$\left(\partial T/\partial r\right)_c$	critical hot spot temperature gradient
a	acoustic speed
r_0	initial hot spot radius
ΔT_0	temperature increase at the hot spot
P_0	initial pressure outside the hot spot
T_0	initial temperature outside the hot spot
ϕ	fuel-air equivalence ratio
u_a	reaction wave speed
x_a	reaction wave position
x_p	pressure wave position

References

[1] Clerk, D., Transactions of the Faraday Society, 1926.
[2] Prochazka, G., Hofmann, P., Geringer, B., Willand, J., Jelitto, C., Schäfer, O., 26. Internationales Wiener Motorensymposium, 2005.
[3] Zeldovich, Y.B., Combust. Flame 39 (1980) 211-214.
[4] Bradley, D., Morley, C., Emerson, D.R., SAE Technical Paper 2002-01-2868, 2002.
[5] Bradley, D., Morley, C., Walmsley, H. L., SAE Technical Paper 2004-01-1970, 2004.
[6] Kalghatgi, G.T., Bradley, D., Int. J. Engine Res. 13 (2012), 399-414.
[7] Rudloff, J., Zaccardi, J-M., Richard, S., Anderlohr, J.M., Proc. Combust. Inst. 34 (2013) 2959-2967.
[8] Robert, A., Richard, S., Colin, O., Poinsot, T., Comb. and Flame 162 (2015) 2788-2807.

[9] Misdariis, A., Vermorel, O., Poinsot, T., Proc. Combust. Inst. 35 (2015) 3001-3008.
[10] Bates, L., Bradley, D., Paczko, G., Peters, N., Comb. and Flame 166 (2016), 80-85.
[11] Gu, X.J., Emerson, D.R., Bradley, D., Combust. Flame 133 (2003) 63–74.
[12] Dai, P., Chen, Z., Chen, S., Ju, Y., Proc. Combust. Inst. 35 (2015) 3045–3052
[13] Zeldovich, Y.B., Librovich, V.B., Makhviladze, G.M., Sivashinsky, G.I., Astronaut. Acta 15 (1970) 313–321.
[14] Colin, O., Da Cruz, A. P., Jay, S., Proc. Combust. Inst. 30 (2005), 2649–2656.
[15] Robert, A., Richard, S., Colin, O., Martinez, L., De Francqueville, L., Proc. Combust. Inst. 35 (2015), 2941–2948.
[16] Péra, C., Knop, V., Fuel 96 (2012), 59-69.
[17] Gourdain, N., Gicquel, L., Staffelbach, G., Vermorel, O., Duchaine, F., Boussuge, J.-F., Poinsot, T., Comput. Sci. Discovery 2(1) (2009) 015004.